*Journal of Fluids and Structures* (2001) **15**, 523–532
doi:10.1006/jfls.2000.0363, available online at http://www.idealibrary.com on IDEAL®

# FORCES AND WAKE MODES OF AN OSCILLATING CYLINDER

J. Carberry, J. Sheridan
*Department of Mechanical Engineering, Monash University*
*Clayton, 3800, Australia*

AND

D. Rockwell
*Department of Mechanical Engineering and Mechanics, Lehigh University*
*Bethlehem, PA 18015, U.S.A.*

(Received 31 August 2000, and in final form 27 November 2000)

This investigation considers the wake states of a cylinder subjected to forced oscillations at frequencies close to the Karman frequency. Two distinctly different wake states are observed. The emphasis is on the transition between these states, which is characterized in terms of the lift force on the cylinder and the instantaneous patterns of vortex structures in the near-wake. As the frequency of oscillation increases, there is simultaneously an abrupt jump in the lift force and a change in the mode of vortex shedding. The jump in the lift force involves a sharp increase in the magnitude of the lift coefficient and a phase shift of the order 180°. The corresponding mode change involves an alteration in both the timing of the vortex initially shed from the cylinder and the overall pattern of vortices in the near-wake. Whilst previously these changes have been observed individually in separate forced vibration investigations, we show conclusive evidence that these two events are intrinsically linked. Moreover, for a narrow band of frequencies, a self-excited transition is possible, where the wake state changes while the cylinder oscillates at a constant frequency. © 2001 Academic Press

## 1. INTRODUCTION

Flow past a stationary cylinder results in organized vortex shedding at a characteristic frequency $f_o$. Controlled excitation of the cylinder at frequencies $f_e$, close to the frequency $f_o$ of the natural instability, results in significant changes in both the wake structure and the forces on the cylinder.

The interaction of a flow field and an oscillating cylinder has received extensive investigation. An early study by Bishop & Hassan (1963) found that, as $f_e/f_o$ increased through unity, the lift force showed a sharp increase in amplitude and a phase "jump" of close to 180°. Similar changes in the lift force have been observed by a number of researchers including Sarpkaya (1995), Gopalkrishnan (1993) and Staubli (1993). Separate studies have shown that there are also significant changes in the vortex patterns of the near-wake around $f_e/f_o = 1$; these investigations have focussed on either qualitative or quantitative visualization. Williamson & Roshko (1988), in their extensive mapping of vortex shedding modes, observed a change in the mode of vortex shedding from 2P to 2S. Changes in the wake have also been described in terms of the timing of the initially formed vortex: Ongoren & Rockwell (1988) and Gu *et al.* (1994) found that as $f_e/f_o$ increased there was a systematic

0889–9746/01/040523 + 10 $35.00/0 © 2001 Academic Press

shortening of the wake, until at a critical $f_e/f_o$ close to unity, there was an abrupt change in the sign of the initial vortex. This change in timing is related to an alteration of the near-wake topology. Furthermore, the near-wake of an oscillating cylinder is directly analogous to the wake from the thick trailing edge of a plate. Staubli & Rockwell (1989) and Lotfy & Rockwell (1993) have defined a change in timing of the initially shed vortex similar to that of the foregoing cases of the wake from a circular cylinder.

A link between the wake mode and forces on the cylinder was established numerically by Blackburn & Henderson (1999). They found that a change of the lift force on the oscillating cylinder was associated with a change in the timing of the initially shed vortex. However, they did not observe the 2P mode of vortex shedding described by Williamson & Roshko (1988). This may have been due to their simulation being two-dimensional, and also at a low amplitude of oscillation and Reynolds number. They also found that, for a given $f_e/f_o$, the wake could exhibit two different states and that these states were not always stable. Staubli & Rockwell (1989) show that, for controlled oscillations of the thick trailing edge of a plate, there is a relationship between the switch in timing of the initially shed vortex and an abrupt change in the phase and magnitude of the lift force determined from pressure measurements.

Both the jump in the properties of the lift force and the change in either the mode of vortex shedding or the sign of the initial vortex, have been observed over a wide range of Reynolds numbers and oscillation amplitudes. While the finer details of these changes may vary with flow parameters such as Re and $A/D$, the abrupt changes described above appear to be a robust feature of these flows. The present work is an experimental investigation of the link between changes in the wake of an oscillating cylinder and the forces on the cylinder. In particular, we focus on patterns of vorticity and their relationship to the amplitude and phase of the unsteady lift.

An interesting aspect of the forced oscillation of a cylinder is how it relates to self-excited vibration induced by vortex shedding. Recently, the elastically mounted cylinder has received considerable attention, particularly for cases with low mass damping. As the reduced velocity is varied, there are abrupt changes in the amplitude of oscillation and the phase of the lift force. These features have allowed the flow to be categorized into different branches, as presented by Khalak & Williamson (1999). Brika & Laneville (1993) found that, as their long vibrating cable moved from the initial branch to the lower branch, there appeared to be a corresponding change in the mode of vortex shedding from 2S to 2P. More recently Govardhan & Williamson (2000) have presented evidence that, as the reduced velocity decreases (analogous to an increase in $f_e/f_o$), the movement of the flow state from the upper or lower branch to the initial branch corresponds to a change in the mode of vortex shedding from 2P to 2S, and a change in the phase of the vortex lift force. They also observed a change in the timing of vortex shedding and therefore a change in the sign of the initially formed vortex. The changes in the forces and wake modes in vortex-induced vibrations appear to have many features in common with the simplified case where the cylinder oscillations are forced.

## 2. EXPERIMENTAL METHOD

The experiments were performed in a free-surface water channel at Lehigh University. The working section had a width of 914 mm, depth 609 mm and was 4928 mm long. The free-stream velocity $U$ was 0·090 m s$^{-1}$ with a turbulence level of less then 0·1%. A schematic of the experimental apparatus is shown in Figure 1. The 317·5 mm long cylinder had a diameter $D$ of 25·4 mm giving an aspect ratio of 12·5. The Reynolds number based on $U$ and $D$ was $2{\cdot}3\times10^3$ and the Kármán frequency, $f_o$, of vortex formation from the corresponding stationary cylinder was 0·748 Hz. A high-resolution stepper motor system

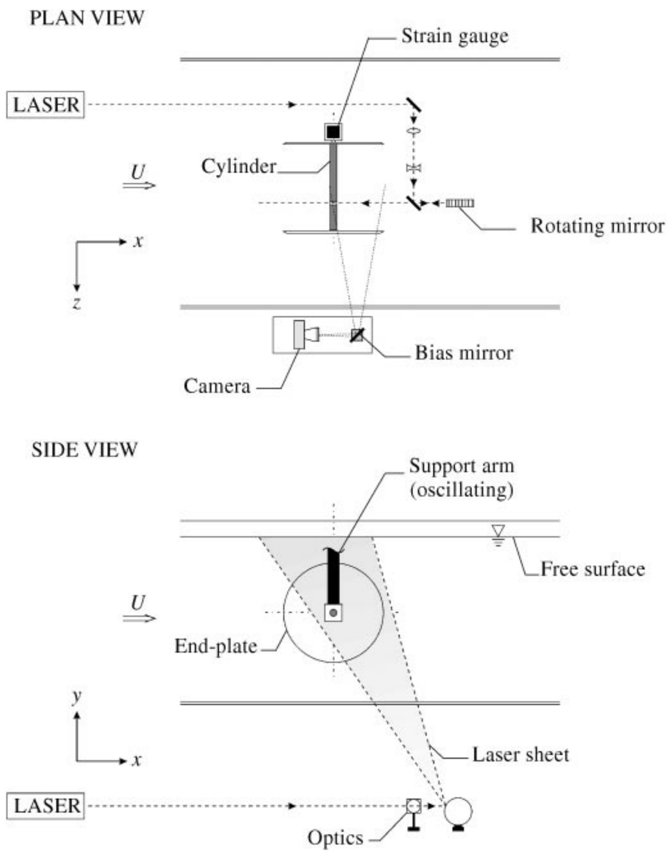


Figure 1. Schematic of experimental system.

was used to oscillate the cylinder transverse to the free stream such that its vertical motion was given by

$$y(t) = A \sin(2\pi f_e t), \tag{1}$$

where $A$ is the amplitude of oscillation and $f_e$ is the frequency of oscillation.

The amplitude of the oscillations was held constant at $A/D = 0{\cdot}5$, while the frequency was varied over the range $0{\cdot}5 \leq f_e/f_o \leq 1{\cdot}4$. For each value of $f_e/f_o$, the cylinder started oscillations from rest at $t = 0$, corresponding to the beginning of the force traces. Following each experiment, the cylinder remained stationary in the free stream for a time equivalent to more then 500 Kármán cycles.

A cross-section of the flow was illuminated by a laser sheet, as shown in Figure 1. A transparent laser window incorporated into the cylinder allowed the laser to illuminate the flow on the opposite side of the cylinder. The velocity field around the cylinder was measured using a laser scanning version of high-image-density particle image velocimetry, described by Rockwell *et al.* (1993). The images were recorded on high-resolution 35 mm film and digitised at 106 pixels/mm. The velocity field was calculated by employing a single-frame cross-correlation technique. An interrogation window of $90 \times 90$ pixels and overlap ratio of 0·50 resulted in a velocity field with 3700 vectors.

The span-averaged forces on the cylinder were measured using strain gauges in a full Wheatstone bridge configuration. For each experiment 5000 data points were sampled at a Nyquist frequency of 6·25 Hz. The inertia forces due to the vertical acceleration of the cylinder were calculated and subtracted from the lift force. For the range of frequencies studied, the wake was "locked-on" to the cylinder oscillation and the dominant frequency in the lift forces was $f_e$. Thus, the lift force can be approximated by a sinusoidal function:

$$\mathrm{Lift}(t) \approx (\tfrac{1}{2}\rho U^2 DL) C_L \sin(2\pi f_e t + \phi_{\mathrm{lift}}), \tag{2}$$

where $C_L$ is the amplitude of the lift coefficient and $\phi_{\mathrm{lift}}$ is the phase with respect to the cylinder displacement, $y(t)$. Both $C_L$ and $\phi_{\mathrm{lift}}$ were calculated in the time domain using data points corresponding to more than 400 cylinder oscillations.

## 3. RESULTS AND DISCUSSION

### 3.1. Relation of Lift Forces to Wake Modes

The amplitude and phase of the lift coefficient are shown as a function of $f_e/f_o$ in Figure 2(a). At low values of $f_e/f_o$, the lift force has a small amplitude and is approximately out-of-phase

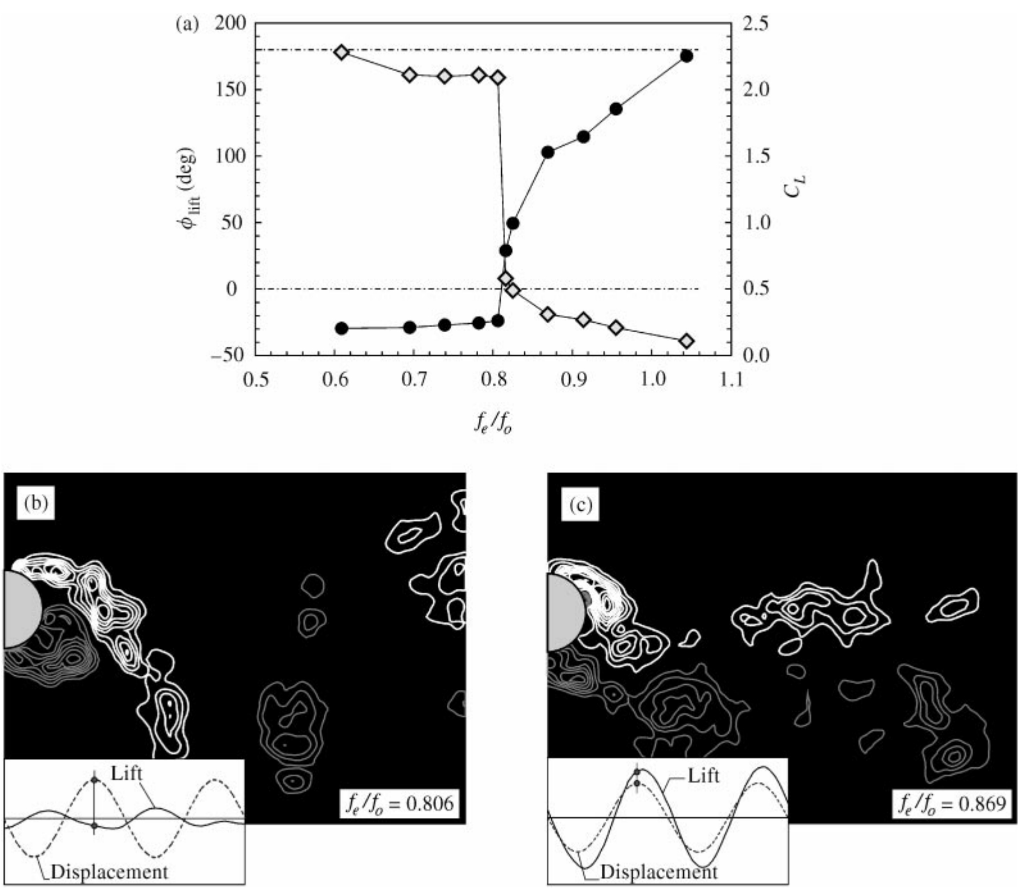


Figure 2. (a) Lift phase, $\phi_{\mathrm{lift}}$, and amplitude of the lift coefficient $C_L$ as a function of frequency ratio $f_e/f_o$, in which $f_e$ is the excitation frequency and $f_o$ is the Kármán frequency: ◇, lift phase; ●, $C_L$. Instantaneous vorticity fields are shown in (b) and (c). The time trace inserts show the instantaneous lift and displacement, where the timing of the image acquisition is indicated by a small circle.

with the cylinder displacement, $y$. As $f_e/f_o$ increases, the lift properties do not vary significantly until $f_e/f_o = 0{\cdot}81$. At this value, there is simultaneously an abrupt increase in $C_L$ and a drop in $\phi_{\text{lift}}$ such that the lift force is approximately in-phase with the cylinder oscillation. The sharp jump in the lift properties has been observed in previous studies: Bishop & Hassan (1963), Sarpkaya (1995), Gopalkrishnan (1993) and Staubli (1993). As $f_e/f_o$ increases further, the lift properties change gradually: $C_L$ increases and $\phi_{\text{lift}}$ decreases. The simultaneous jump in $C_{\text{L}}$ and $\phi_{\text{lift}}$ is indicative of significant changes in the cylinder wake. The sharp change in the lift properties is referred to herein as a transition from a low-frequency lift force to high-frequency lift force. The properties of the lift force can now be associated with either low frequencies before transition, or high frequencies after transition. Before transition, $C_L$ is small and $\phi_{\text{lift}}$ is large, while after transition $C_L$ is large and $\phi_{\text{lift}}$ is small, and generally negative.

The value of the lift phase indicates the direction of energy transfer between the cylinder and the fluid. When $0 < \phi_{\text{lift}} < 180°$, there is positive energy transfer from the fluid to the cylinder. The oscillation of an elastically mounted cylinder requires positive energy transfer to the cylinder and therefore the lift phase is restricted to values $0 \le \phi_{\text{lift}} \le 180°$. However, when the cylinder is forced to oscillate, all values of $\phi_{\text{lift}}$ are physically possible. For the case presented here, the direction of energy transfer went from positive to negative as $\phi_{\text{lift}}$ passed though $0°$. Generally speaking, for forced oscillations, the value of $\phi_{\text{lift}}$, and therefore the direction of energy transfer, may also depend on Re and $A/D$.

We now consider transition in terms of the structure of the near-wake. The instantaneous vorticity fields in Figure 2(b, c) show the wake structure for values of $f_e/f_o$ on either side of transition. The images, both acquired at the top of the cylinders oscillation cycle, show two distinctly different wakes. Figure 2(b) is representative of the wake mode at low frequencies before transition, while Figure 2(c) is representative of the wake mode after transition. Comparing the two cases, we see that the vortex structures in the near-wake are of opposite sign. At $f_e/f_o = 0{\cdot}806$ a negative vortex structure is formed from the attached shear layer and a positive initial vortex forms close to the cylinder. After transition, at $f_e/f_o = 0{\cdot}869$, the structure that is shed into the wake is positive and the initial vortex is negative. The change in sign of the vortex structures is consistent with the shift of approximately 180° in the lift phase. In the present investigation, a similar change in timing was also evident at lower amplitudes of oscillation; however, in these cases the formation of the 2P wake mode was not well defined. This finding is consistent with previous work at low amplitudes, including that of Gu *et al.* (1994) and will be reported in a forthcoming publication.

We now consider in more detail the wake modes on either side of the transition region. Figure 3 shows the time evolution of the vortex structures during the downwards stroke of the cylinder. At the top of the oscillation, the low-frequency wake ($f_e/f_o = 0{\cdot}806$) has a long negative vortex structure extending across the back of the cylinder and into the lower half of the wake. However, at the same phase of the oscillation cycle the attached negative vorticity in the high frequency wake ($f_e/f_o = 0{\cdot}869$) takes the form of a small concentrated structure at the back of the cylinder. As the cylinder moves downwards, the negative vorticity in the low-frequency wake is shed as two separate structures. The vorticity from the end of the attached shear layer is shed into the lower half of the wake and forms a counter-rotating pair with previously shed vorticity. The negative vorticity closer to the cylinder is shed into the upper wake, and eventually forms a second counter-rotating pair during the next half-cycle. Thus, the vorticity forms two counter-rotating pairs per cycle, which is commonly described as the 2P mode of shedding. However, the mode of vortex shedding in the high-frequency wake is clearly different. As the cylinder moves downwards, a single positive vortex is shed. In the next half-cycle, the shedding of a single negative vortex results in the classical Karman, or 2S, mode of shedding. At the transition from the low-frequency state to

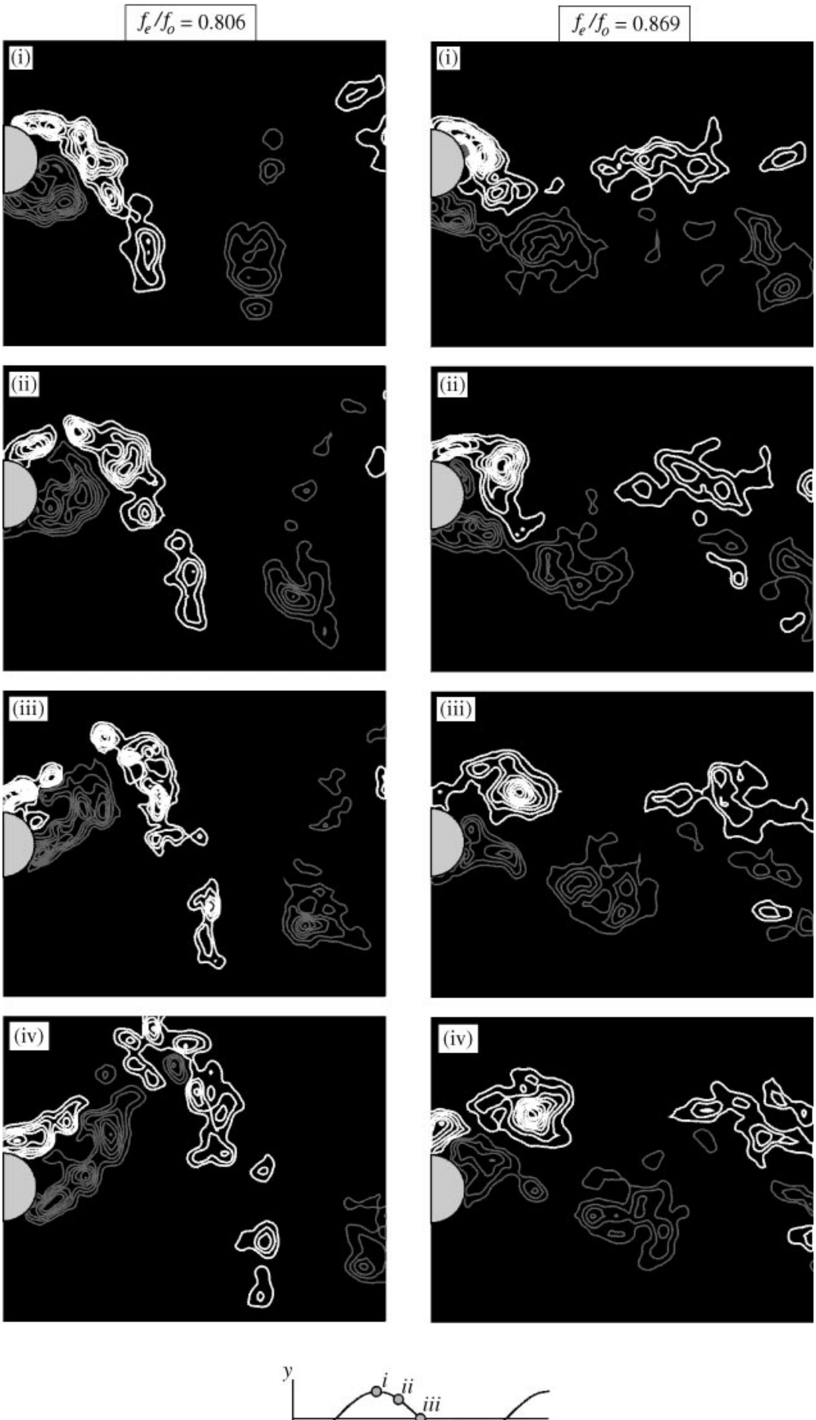


Figure 3. The evolution of vortex structures during the downward stroke of the cylinder. The left-hand side column shows the low-frequency wake mode before transition ($f_e/f_o = 0{\cdot}806$), while the high-frequency wake mode after transition ($f_e/f_o = 0{\cdot}869$) is on the right. The position of the cylinder for each image is shown in the displacement inserts beneath the fields.

the high-frequency state, we observed not only a change in the timing of vortex shedding, but also a change in the mode of vortex shedding.

The two modes of vortex shedding generate significantly different distributions of vorticity downstream of the cylinder. In the high-frequency wake, negative vorticity is found predominantly in the upper half of the wake, while the lower wake is dominated by positive vorticity. However, for the low-frequency wake, vorticity of both signs is found throughout the vertical extent of the wake.

The wake states either side of transition can now be described in terms of both the lift force and the structure of the near-wake. For the low-frequency wake state, $C_L$ is small and $\phi_{\text{lift}}$ is large, while the structure of the near wake is characterized by the wake shown in Figure 2(b), with a positive initial vortex. Whilst for the high-frequency wake state $C_L$ is large, $\phi_{\text{lift}}$ is small and the near-wake structure is characterized by the wake in Figure 2(c).

### 3.2. Transition

In order to understand the nature of the transition between wake states we focused on frequencies close to transition. Representative images are shown in Figure 4. At each value of $f_e/f_o$, the wake state at $t = 0$ is that of a stationary cylinder in a free stream. For $t > 0$ the cylinder oscillates at a constant frequency and the oscillating wake appears to be fully established in less than 10 oscillations. For a narrow band of frequencies close to transition, after many oscillations, self-excited changes were observed in the lift properties. We will now show that these changes correspond to a self-excited transition from the low-frequency state to the high-frequency state.

The lift trace for a typical self-excited transition is shown in Figure 4(a). The corresponding instantaneous values of the amplitude and phase of the lift coefficient are shown in Figure 4(b). In this example, the transition begins after more than 150 oscillation cycles. For time less than 97 s the lift forces are consistent with the low-frequency state described previously: the lift coefficient is of small amplitude and the lift phase is large. Conversely, for times after 128 s the lift force is consistent with the high-frequency wake state. In-between these two states is a transient transition region where the lift force is not consistent with either state. The expanded time trace in Figure 4(c) shows the changing relationship between the lift and displacement within the transition region.

It is expected that the self-excited transition in the magnitude and phase of the lift coefficient corresponds to a change in the structure of the near-wake. The wake patterns in both Figures 4(d) and (e) were acquired at the top of the oscillation cycle, at the times indicated on the lift trace. These images are representative of the wake structures either side of the self-excited transition. Despite the fact that the oscillation frequency is constant, these wake states are clearly different. The wake structure shown in Figure 4(d) corresponds to values of lift magnitude and phase that are consistent with the low-frequency state. The wake is shedding in the 2P mode and is clearly consistent with the steady-state low-frequency state, described in conjunction with Figure 2(b). Similarly, Figure 4(e) correlates well with the steady-state high-frequency wake mode of Figure 2(c). Thus, the wake states either side of the self-excited transition are consistent with the wake states at much lower and higher frequencies.

For the self-excited transition, the instantaneous magnitude and phase of the lift coefficient change smoothly from their low-frequency values to high-frequency values. However, within this transition region we observe that the change in $\phi_{\text{lift}}$ occurs slightly before the change in $C_L$. After transition, there is some variation in the magnitude and phase of the lift coefficient, which was not observed at higher values of $f_e/f_o$. During this variation, there is a clear inverse relationship between the instantaneous values of $C_L$ and $\phi_{\text{lift}}$; however, once

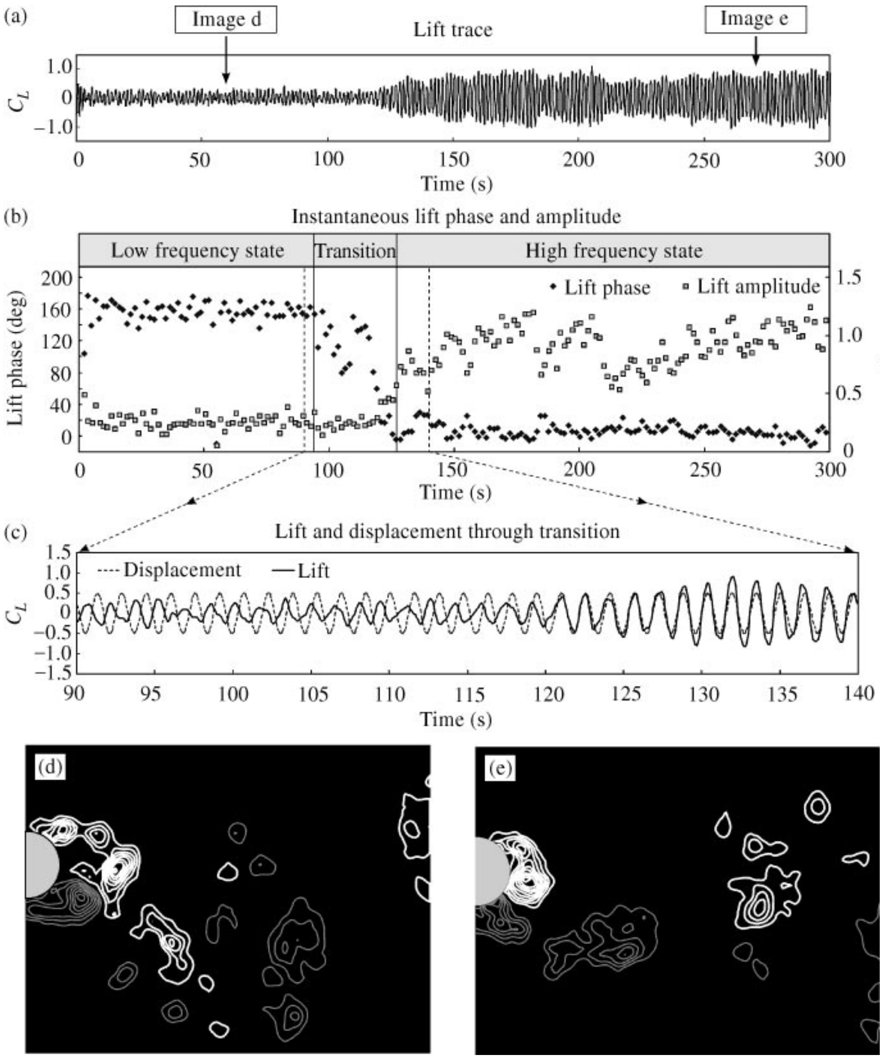


Figure 4. The lift time trace (a) shows a self-excited transition occurring after more then 150 oscillations cycles at a constant excitation frequency of $f_e/f_o = 0{\cdot}815$. The corresponding variation in the instantaneous values of the lift phase and amplitude of the lift coefficient are shown in (b). The lift and displacement traces during the transition are shown in more detail in (c). The wake modes on either side of the self-excited transition are shown at $t = 60$ s corresponding to image (d), and at $t = 270$ s represented as image (e). Both images were acquired at the top of the oscillation cycle.

the high-frequency state was established by a self-excited transition, a return to the low-frequency state was never observed.

## 4. CONCLUSIONS

In this paper we have described a transition between two wake states which exhibit distinctly different lift forces and wake modes. The interaction between the natural instability of the wake and the forced oscillation plays an important role and the flow properties depend strongly on $f_e/f_o$. At values of $f_e/f_o$ close to unity the changing relationship between these instabilities results in an abrupt change in the wake state.

Our investigation showed that changes in the lift force are intrinsically related to changes in the structure of the near-wake. As $f_e/f_o$ increased there was a transition from a small amplitude lift force, which was approximately out-of-phase with the cylinder oscillations, to a large amplitude in-phase lift force. Simultaneously, there was a change in the sign of the initial vortex and the mode of vortex shedding went from 2P to 2S. The change in the mode of vortex shedding appears to be related to the change in the timing of vortex formation, which is in turn related to the shift in the lift phase. For forced oscillations of the cylinder over a wide range of amplitudes, further consideration should be given to the occurrence of a change in timing of the initially shed vortex as a consistent requirement for the jump in the lift properties, as well as its relationship to the occurrence of, and transition between, the 2P and 2S modes.

For a narrow band of $f_e/f_o$, we observed a self-excited transition at a constant frequency of oscillation. Immediately following start-up, the lift force and wake mode conformed to the low-frequency wake state. After a number of oscillations, the lift force and wake mode changed smoothly until they were both consistent with the high-frequency wake state. The self-excited transition depends on the relative stability of three wake states: the low- and high-frequency wake states and also the wake state of the stationary cylinder before start-up. Therefore, the existence of this self-excited transition and the way in which it occurs may also depend on flow parameters such as $A/D$ and Re.

## ACKNOWLEDGEMENTS

Primary support for this research program was provided by the Office of Naval Research Grant N00014-94-1-0815, P0006, monitored by Dr Thomas Swean, and by the Australian Research Council through the ARC Large Grant A89702238. In addition, supplemental support was provided by NSF Grant CTS-9803734. Ms Carberry acknowledges support through an Australian Postgraduate Award. The authors gratefully acknowledge this financial support.

## REFERENCES

BISHOP, R. E. D. & HASSAN, A. Y. 1963 The lift and drag forces on a circular cylinder in a flowing fluid. *Proceedings of Royal Society* (*London*) A **277,** 32–50.

BLACKBURN, H. M. & HENDERSON, R. D. 1999 A study of two-dimensional flow past an oscillating cylinder. *Journal of Fluid Mechanics* **385,** 255–286.

BRIKA, D. & LANEVILLE, A. 1993 Vortex-induced vibrations of a long flexible circular cylinder. *Journal of Fluid Mechanics* **250,** 481–508.

GOPALKRISHNAN R. 1993 Vortex induced forces on oscillating bluff cylinders. Ph.D. thesis, Massachusetts Institute of Technology, Cambridge, MA, U.S.A.

GOVARDHAN, R. & WILLIAMSON, C. H. K. 2000 Modes of vortex formation and frequency response of a freely vibrating cylinder. *Journal of Fluid Mechanics* **420,** 85–130.

GU, W., CHYU, C. & ROCKWELL, D. 1994 Timing of vortex formation from an oscillating cylinder. *Physics of Fluids* **6,** 3677–3682.

KHALAK, A & WILLIAMSON, C. H. K. 1999 Motions, forces and mode transitions in vortex-induced vibrations at low mass-damping. *Journal of Fluids and Structures* **13,** 813–851.

LOTFY, A. & ROCKWELL, D. 1993 The near-wake of an oscillating trailing edge: mechanisms of periodic and periodic response. *Journal of Fluid Mechanics* **251,** 173–201

ONGOREN, A. & ROCKWELL, D. 1988 Flow structure from an oscillating cylinder Part1. Mechanisms of phase shift and recovery in the near wake. *Journal of Fluid Mechanics* **191,** 197–223.

ROCKWELL, D., MAGNESS, C., TOWFIGHTI, J., AKIN, O. & CORCORAN, T. 1993 High image-density particle image velocimetry using laser scanning techniques. *Experiments in Fluids* **14,** 181–192.

SARPKAYA, T. 1995 Hydrodynamic damping, flow-induced oscillations, and biharmonic response. *ASME Journal of Offshore Mechanics and Artic Engineering* **177,** 232–238.

Staubli, T. 1993 Untersuchung der oszillierenden Kräfte am querangeströmten, schwingenden Kreiszylinder. Dissertation ETH 7322.
Staubli, T. & Rockwell, D. 1989 Pressure fluctuations on an oscillating trailing edge. *Journal of Fluid Mechanics* **203,** 307–346
Williamson, C. H. K. & Roshko, A. 1988 Vortex formation in the wake of an oscillating cylinder. *Journal of Fluids and Structures* **2,** 355–381.